

Supplementary Materials

Mesoporous Dual-Semiconductor ZnS/CdS Nanocomposites as Efficient Visible Light Photocatalysts for Hydrogen Generation

Ioannis Vamvasakis ^{1,*}, Evangelos K. Andreou ¹ and Gerasimos S. Armatas ¹

¹ University of Crete, Department of Materials Science and Technology, 70013 Voutes, Heraklion, Greece.

* Correspondence: j.vamvasakis@gmail.com; Tel.: 0030-2810-545119.

Supporting Tables

Table S1. Chemical composition of the as-prepared mesoporous CdS and ZnS NCAs, along with the mesoporous ZnS/CdS nanocomposites with different ZnS content, according to EDS analysis. The EDS results for the reference materials ZnS/CdS bulk and RNAs with 50 wt.% ZnS content are also shown.

Sample	Cd (at.%)	Zn (at.%)	S (at.%)	ZnS content ¹ (wt.%)
CdS NCAs	50.73 ± 0.25	0	49.27 ± 0.25	0
10-ZnS/CdS	43.16 ± 0.49	7.08 ± 0.40	49.76 ± 0.58	9.96 ± 0.23
30-ZnS/CdS	27.24 ± 0.15	16.93 ± 0.71	55.83 ± 0.67	29.54 ± 0.44
50-ZnS/CdS	17.67 ± 0.19	26.58 ± 0.65	55.75 ± 0.51	50.37 ± 0.20
70-ZnS/CdS	9.62 ± 0.19	34.76 ± 0.59	55.62 ± 0.57	70.91 ± 0.03
90-ZnS/CdS	4.03 ± 0.17	46.81 ± 0.91	49.16 ± 0.55	88.70 ± 0.13
ZnS NCAs	0	53.65 ± 0.33	46.35 ± 0.33	100
ZnS/CdS bulk ²	21.11 ± 0.51	31.31 ± 1.28	47.58 ± 0.92	50.02 ± 0.24
ZnS/CdS RNAs ³	17.93 ± 0.10	26.39 ± 0.40	55.68 ± 0.39	49.82 ± 0.14
50-ZnS/CdS AC ⁴	15.62 ± 0.26	23.42 ± 0.60	60.96 ± 0.30	50.29 ± 0.10
50-ZnS/CdS-c ⁵	17.47 ± 0.21	31.83 ± 0.53	50.70 ± 0.52	55.14 ± 0.11

¹ As determined on the basis of the EDS Zn and Cd atomic ratios. ² EDS results for the ZnS/CdS bulk reference sample (50 wt.% ZnS). ³ EDS results for the reference material ZnS/CdS RNAs (RNAs: random NC-aggregates) with 50 wt.% ZnS, synthesized through a template-free oxidative coupling of ZnS and CdS NCs. ⁴ EDS results for the 50-ZnS/CdS catalyst retrieved after 24 h of photocatalytic stability test (reaction conditions: 20 mg of catalyst dispersed in a 1.4 M Na₂S and 1.0 M Na₂SO₃ aqueous electrolyte, irradiated with visible light using a 300 W Xe light with a cut-off filter allowing $\lambda \geq 420$ nm). ⁵ EDS results for the 50-ZnS/CdS catalyst retrieved after the photocatalytic corrosion experiment with triethanolamine (TEOA) as hole scavenger (reaction conditions: 20 mg of catalyst dispersed in aqueous solution containing 10% v/v TEOA, irradiated for 3 h under visible light using a 300 W Xe light with a cut-off filter allowing $\lambda \geq 420$ nm).

Table S2. Comparison of H₂-production activities between mesoporous 50-ZnS/CdS and other reported CdZnS-based photocatalysts.

Sample	Reaction conditions	Light source	H ₂ evolution rate (mmol g ⁻¹ h ⁻¹)	Apparent quantum yield (AQY)	Ref.
ZnS/Zn _{1-x} Cd _x S/CdS	5 mg catalyst 0.35 M Na ₂ S & 0.25 M Na ₂ SO ₃ (100 mL)	300 W Xe lamp $\lambda \geq 420$ nm	106.5	-	[1]

CdS/ZnS nanorods	1 mg catalyst 0.75 M Na ₂ S & 1.05 M Na ₂ SO ₃ (20 mL)	300 W Xe lamp $\lambda \geq 420$ nm	239 ($\mu\text{mol h}^{-1} \text{mg}^{-1}$)	16.8% (420 nm)	[2]
0.5%Ru/(CdS) _{0.8} /(ZnS) _{0.2} nanoparticles	150 mg catalyst 0.1 M Na ₂ S & 0.2 M Na ₂ SO ₃ (150 mL)	300 W Xe lamp $\lambda \geq 420$ nm	12.65	-	[3]
Pt-ZnS/CdS 2D/1D nanocomposites	50 mg catalyst ~10% v/v lactic acid (230 mL)	300 W Xe lamp $\lambda > 400$ nm	26	5.7% (420 nm)	[4]
(CdS) _{0.4} /(ZnS) _{0.6}	50 mg catalyst 0.1 M Na ₂ S & 0.1 M Na ₂ SO ₃ (100 mL)	300 W Xe lamp $\lambda \geq 420$ nm	0.83	-	[5]
Zn/Cd-MOF derived ZnS/CdS heterojunction	20 mg catalyst 35 mM Na ₂ S & 18 mM Na ₂ SO ₃ (100 mL)	300 W Xe lamp $\lambda \geq 420$ nm	2.35	3.92% (420 nm)	[6]
Pt-PdS-CdS/ZnS core/shell NCs	1.5 mg catalyst 0.1 M Na ₂ S (50 mL)	300 W Xe lamp $\lambda \geq 380$ nm	~50	-	[7]
PdS-CdS/ZnS core/shell particles	100 mg catalyst 0.1 M Na ₂ S & 0.1 M Na ₂ SO ₃ (270 mL)	300 W Xe lamp $\lambda \geq 400$ nm	2.08	-	[8]
CdS/ZnS core/shell nanorods	10 mg catalyst 0.5 M Na ₂ S & 0.5 M Na ₂ SO ₃ (100 mL)	300 W Xe lamp AM 1.5G	24.1	9.3% (420 nm)	[9]
CdS/ZnS core/shell particles	5 mg catalyst 0.1 M Na ₂ S & 0.1 M Na ₂ SO ₃ (50 mL)	20 W LED $\lambda = 420$ nm	16	8.78% (420 nm)	[10]
CdS/ZnS-NiS microstructures	10 mg catalyst 0.35 M Na ₂ S & 0.25 M Na ₂ SO ₃ (25 mL)	225 W Xe lamp $\lambda \geq 320$ nm	60.44	23.3% (365 nm)	[11]
ZnS-CuS-CdS particles	100 mg catalyst 0.35 M Na ₂ S & 0.25 M Na ₂ SO ₃ (150 mL)	150 W Xe lamp AM 1.5G	0.84	-	[12]
Cd _{0.5} Zn _{0.5} S nano-twins	100 mg catalyst 0.35 M Na ₂ S & 0.25 M Na ₂ SO ₃ (180 mL)	300 W Xe lamp $\lambda > 430$ nm	17.9	43% (425 nm)	[13]

Cd _{0.5} Zn _{0.5} S twined nanorods	100 mg catalyst 0.35 M Na ₂ S & 0.25 M Na ₂ SO ₃ (180 mL)	300 W Xe lamp $\lambda > 430$ nm	25.8	62% (425 nm)	[14]
50-ZnS/CdS NCAs	20 mg catalyst 1.4 M Na₂S & 1.0 M Na₂SO₃ (20 mL)	300 W Xe lamp $\lambda \geq 420$ nm	29.0	60% (420 nm)	This work

Table S3. EIS equivalent circuit fitted parameters for the mesoporous CdS and ZnS NCAs and the as-prepared ZnS/CdS materials.

Sample	R _s (Ohm)	C _{dl} (F)	R _{ct} (Ohm)	[x ²] ¹
CdS NCAs	14.2	63.3 × 10 ⁻⁶	1312	2.1 × 10 ⁻⁴
10-ZnS/CdS	12.7	24.2 × 10 ⁻⁵	686	2.3 × 10 ⁻⁴
30-ZnS/CdS	17.4	17.9 × 10 ⁻⁵	474	4.3 × 10 ⁻⁴
50-ZnS/CdS	12.1	19.5 × 10 ⁻⁵	285	8.7 × 10 ⁻⁴
70-ZnS/CdS	13.4	76.8 × 10 ⁻⁶	486	2.0 × 10 ⁻⁴
90-ZnS/CdS	12.3	86.5 × 10 ⁻⁶	747	4.2 × 10 ⁻⁴
ZnS NCAs	18.0	11.4 × 10 ⁻⁵	1362	2.5 × 10 ⁻⁴
ZnS/CdS bulk ²	9.6	62.5 × 10 ⁻⁶	1499	10.3 × 10 ⁻⁴

¹In EIS analysis, the fitting error is often expressed using the chi-square metric. Typically, a satisfactory fit corresponds to chi-square values ranging from 10⁻² to 10⁻⁴. ²EIS results for the ZnS/CdS bulk reference catalyst (50 wt.% ZnS).

Table S4. PL lifetime biexponential decay model fitting parameters and calculated average lifetimes for the mesoporous CdS and 50-ZnS/CdS NCAs, and the ZnS/CdS bulk analogue with 50 wt.% ZnS.

Catalyst	A ₁ (%)	τ ₁ (ns)	A ₂ (%)	τ ₂ (ns)	τ _{av} (ns)
CdS NCAs	72.5	0.80 ± 0.006	27.5	4.35 ± 0.039	3.20 ± 0.017
50-ZnS/CdS	65.0	1.00 ± 0.012	35.0	4.73 ± 0.055	3.70 ± 0.025
ZnS/CdS bulk	68.5	0.70 ± 0.005	31.5	4.08 ± 0.026	3.16 ± 0.011

¹The average lifetime (τ_{av}) was calculated by the equation: τ_{av} = (Σ_i A_i τ_i²) / (Σ_i A_i τ_i) (i = 1, 2).

Supporting Figures

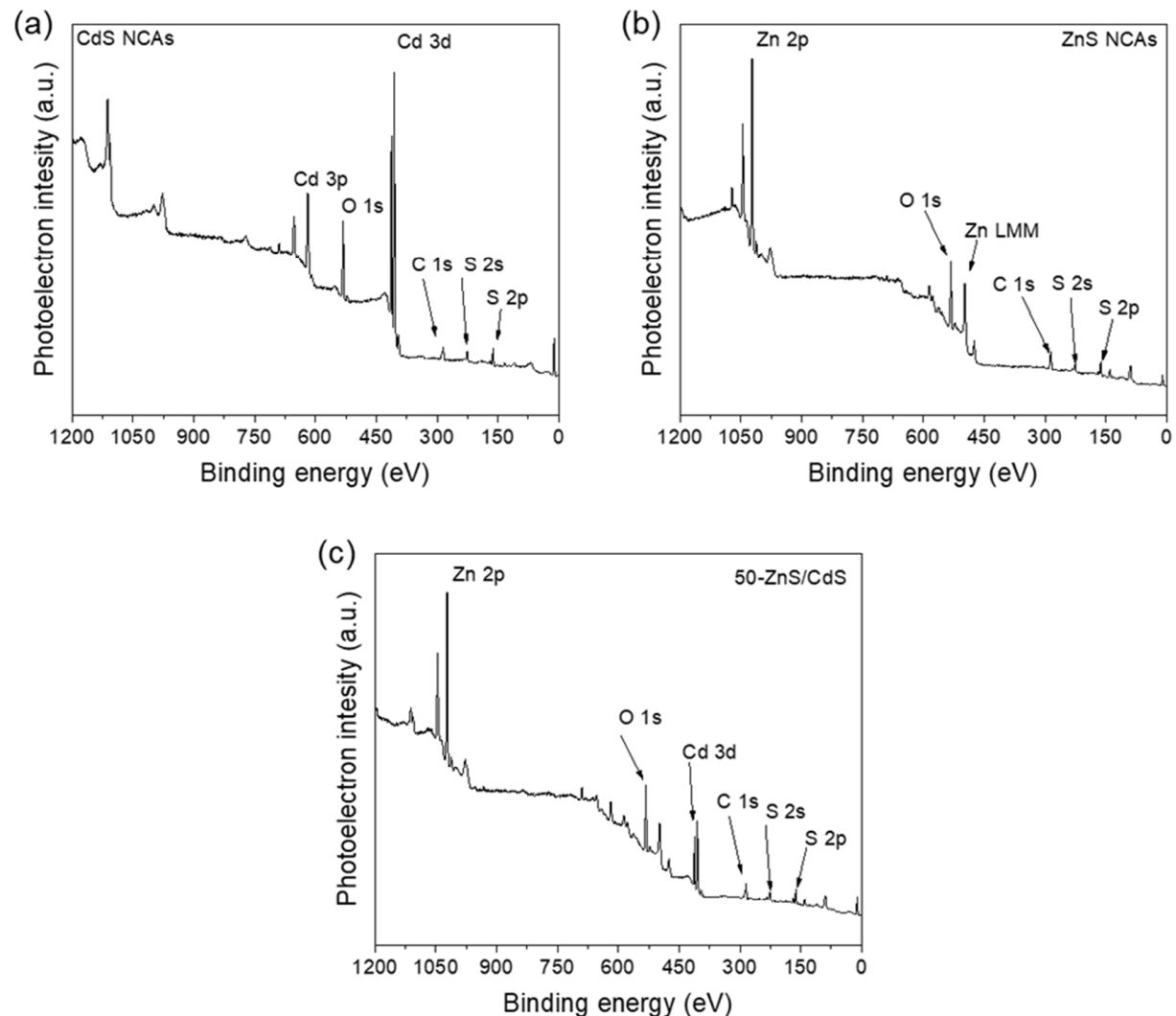


Figure S1. Typical XPS survey spectra of CdS, ZnS and 50-ZnS/CdS NCAs showing the presence of Cd, Zn and S, from the constituent NCs and C and O from adsorbed molecules.

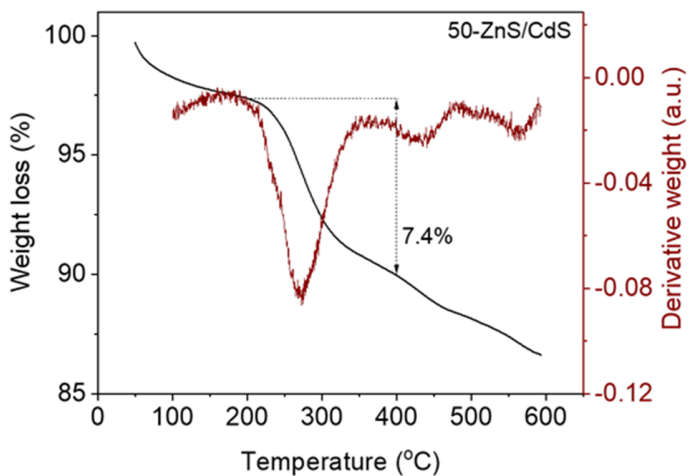


Figure S2. Example of TGA profile for the mesoporous (black line) 50-ZnS/CdS nanocomposite obtained after three cycles of ethanol/water washing process. The weight loss in this sample indicated by the corresponding differential thermogravimetric (DTG) curve (red line) is attributed to the decomposition of organic matter.

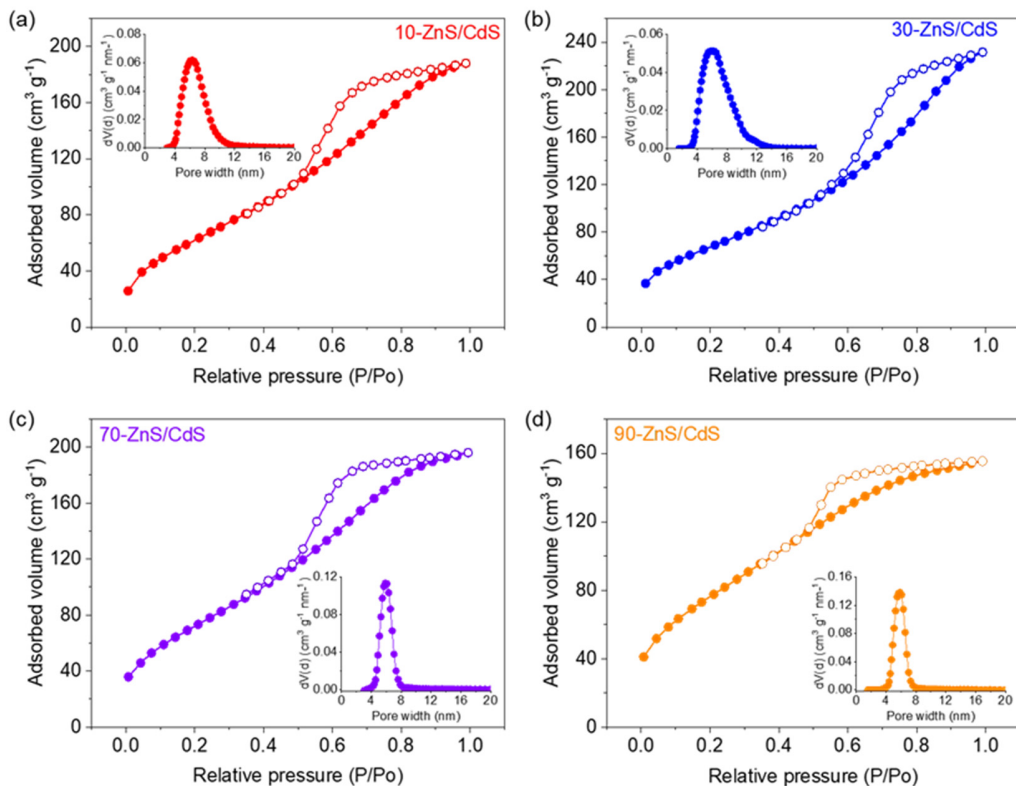


Figure S3. Nitrogen adsorption (filled cycles) and desorption (open cycles) isotherms at $-196\text{ }^{\circ}\text{C}$ for the mesoporous ZnS/CdS nanocomposites featuring different ZnS loadings: (a) 10 wt.%, (b) 30 wt.%, (c) 70 wt.%, and (d) 90 wt.%. Insets: The corresponding NLDFT pore size distributions calculated from the adsorption branch of isotherms.

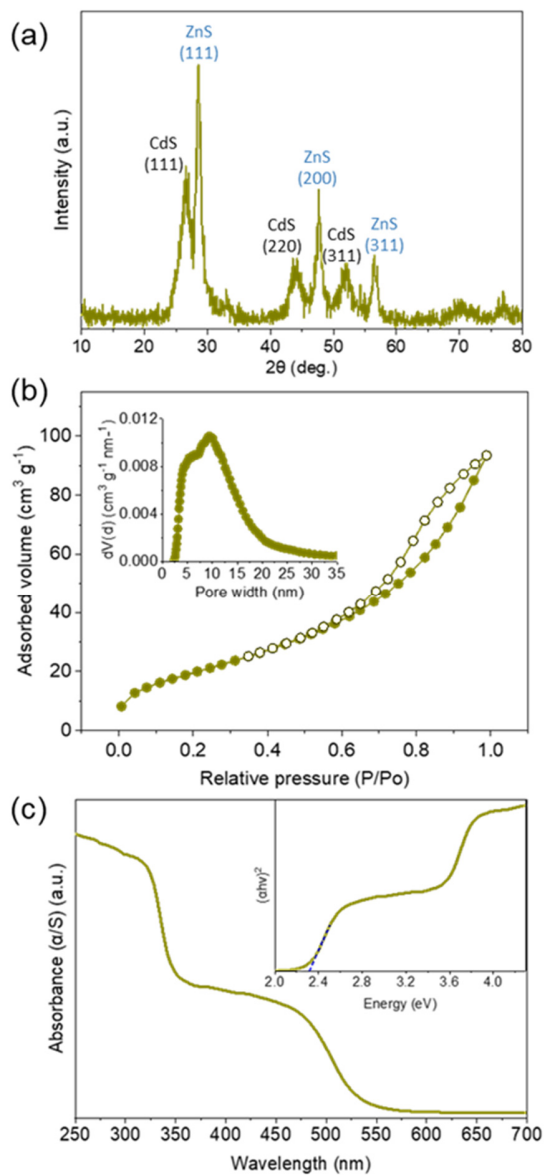


Figure S4. (a) XRD pattern, (b) N₂ adsorption (filled cycles) and desorption (open cycles) isotherms at -196°C and the corresponding NLDFT pore-size distribution plot (inset), and (d) optical absorption spectrum and Tauc plot (inset) of the reference ZnS/CdS bulk catalyst with 50 wt.% ZnS content.

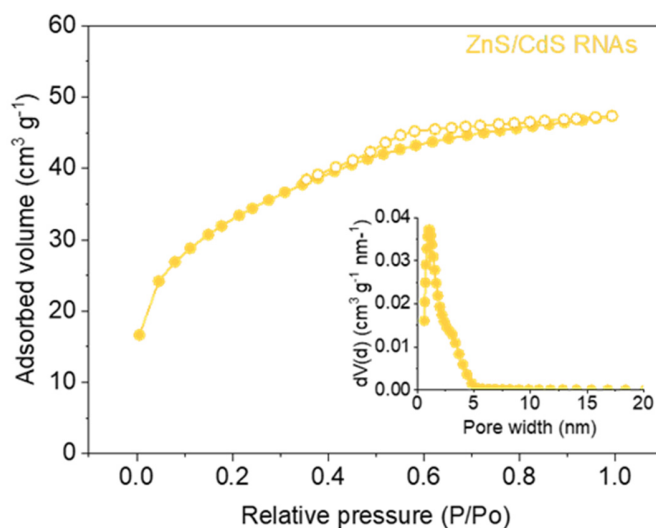


Figure S5. N_2 adsorption (filled cycles) and desorption (open cycles) isotherms at -196°C and the corresponding NLDFT pore-size distribution plot (inset) of the reference ZnS/CdS RNAs catalyst with 50 wt.% ZnS content. Analysis of the adsorption data with the BET method gives a surface area of $114 \text{ m}^2 \text{ g}^{-1}$ and total pore volume of $0.07 \text{ cm}^3 \text{ g}^{-1}$. The NLDFT pore size distribution calculated from the adsorption branch of isotherms indicates a pore size of $\sim 1.5 \text{ nm}$.

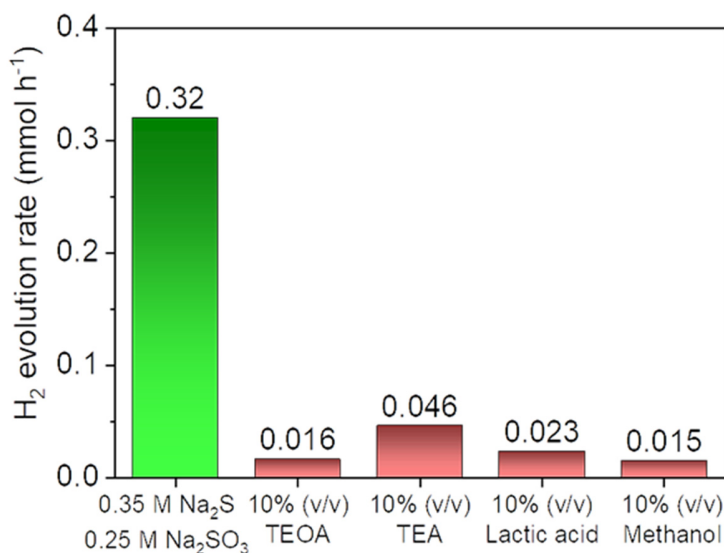


Figure S6. Photocatalytic H_2 evolution rates (averaged over 3-h reaction period) for the mesoporous 50-ZnS/CdS catalyst using different sacrificial reagents: $0.35 \text{ M Na}_2\text{S}$ and $0.25 \text{ M Na}_2\text{SO}_3$, triethanolamine (TEOA, 10% v/v), triethylamine (TEA, 10% v/v), lactic acid (10% v/v) and methanol (10% v/v). All photocatalytic reactions were performed as follows: 20 mg of catalyst dispersed in a 20 mL aqueous solution containing the sacrificial reagent; 300 W Xe light irradiation with a long-pass cut-off filter allowing $\lambda \geq 420 \text{ nm}$.

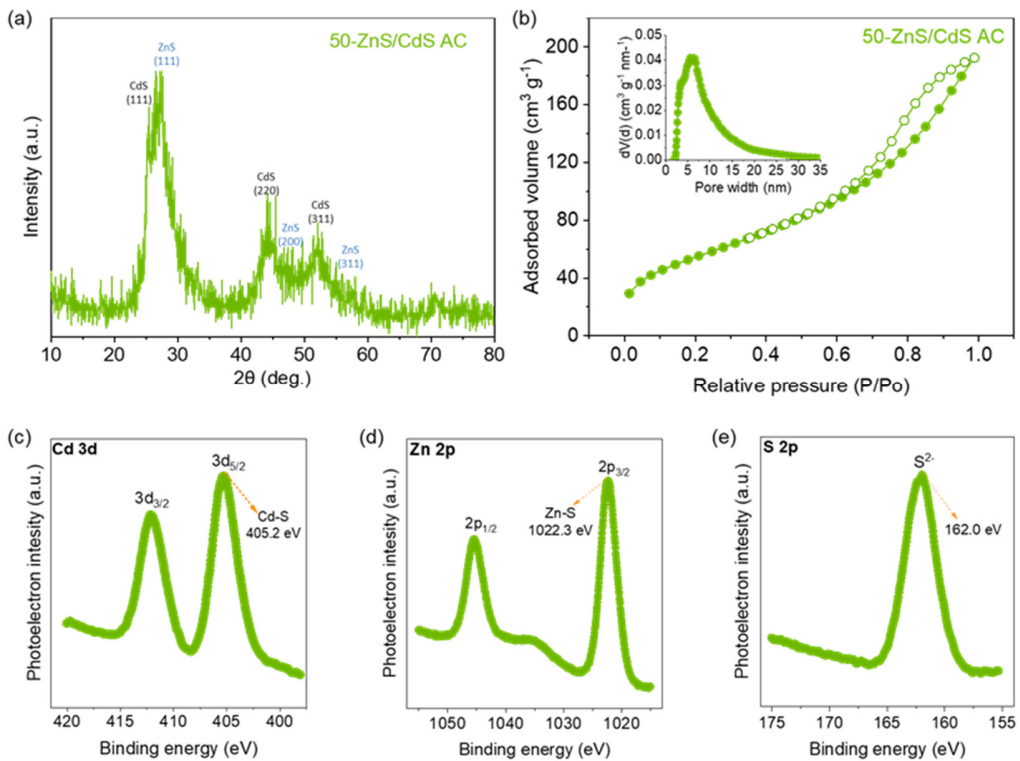


Figure S7. (a) XRD pattern, (b) N₂ adsorption (filled cycles) and desorption (open cycles) isotherms at -196°C (inset: the corresponding NLDFT pore-size distribution plot), and (c-e) typical XPS spectra of the (c) Cd 3d, (d) Zn 2p, and (e) S 2p regions of the 50-ZnS/CdS catalyst retrieved after 24-h of photocatalytic reaction.

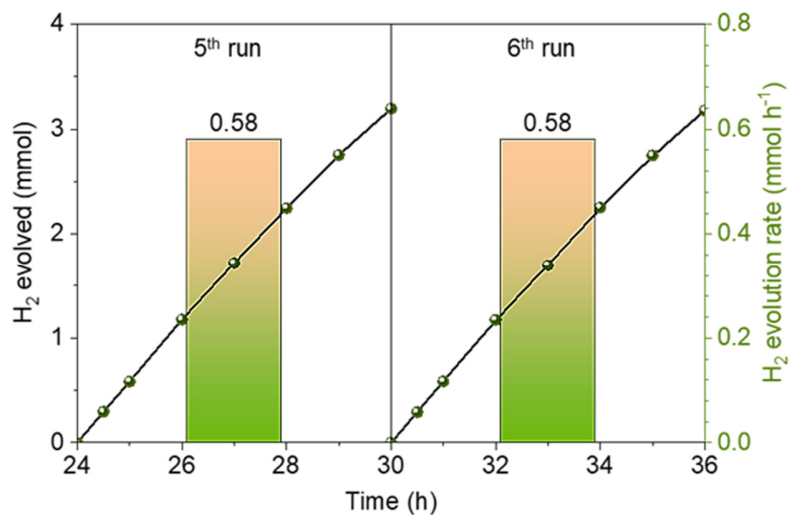


Figure S8. 5th and 6th run of the photocatalytic recycling study of the 50-ZnS/CdS catalyst in a 1.4 M Na₂S and 1.0 M Na₂SO₃ aqueous electrolyte. All the H₂-evolution rates obtained as an average over the initial 3-h reaction period. Reaction conditions: 20 mg catalyst dispersed in 20 mL of fresh electrolyte solution, 300 W Xenon light irradiation with a UV cutoff filter ($\lambda \geq 420 \text{ nm}$), $T = 20 \pm 2^\circ\text{C}$.

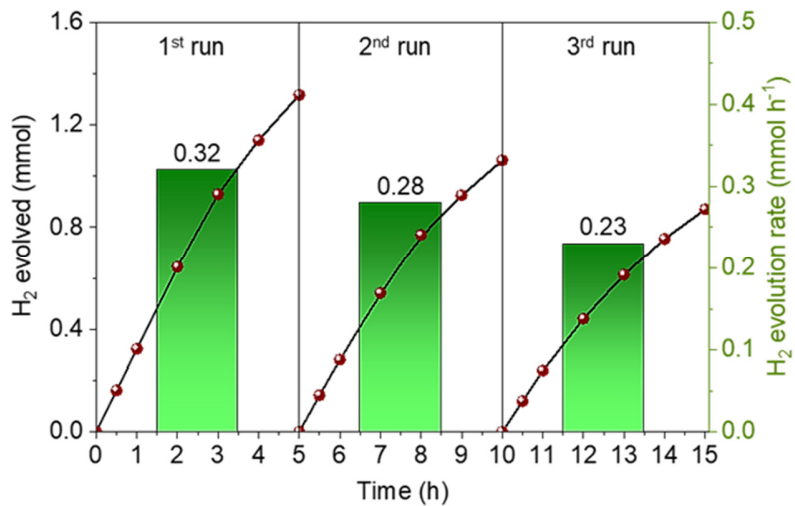


Figure S9. Photocatalytic recycling tests of the 50-ZnS/CdS catalyst in a 0.35 M Na₂S and 0.25 M Na₂SO₃ aqueous electrolyte. All the H₂-evolution rates obtained as an average over the initial 3-h reaction period. Reaction conditions: 20 mg catalyst dispersed in 20 mL of fresh electrolyte solution, 300 W Xenon light irradiation with a UV cutoff filter ($\lambda \geq 420$ nm), T = 20 ± 2 °C.

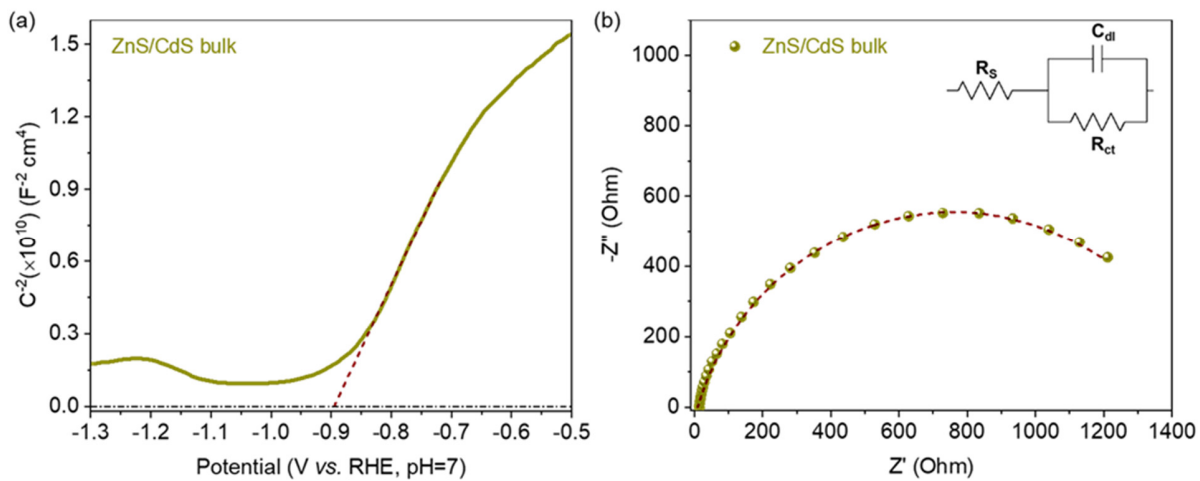


Figure S10. (a) Mott-Schottky plot and (b) EIS Nyquist spectrum (inset: equivalent circuit model) for the reference ZnS/CdS bulk catalyst with 50 wt.% ZnS content.

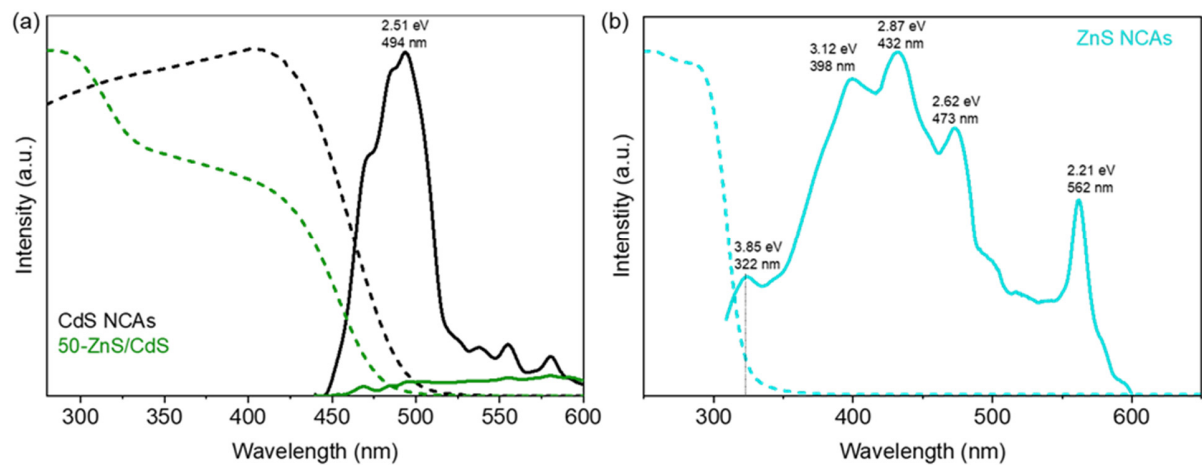


Figure S11. Room-temperature PL emission spectra (solid lines) of (a) mesoporous CdS and 50-ZnS/CdS NCAs (excitation wavelength 380 nm) and (b) mesoporous ZnS NCAs (excitation wavelength 280 nm). The dashed lines correspond to the UV-Vis/NIR absorption spectra of the respective samples.

References

1. Li, K.; Chen, R.; Li, S.L.; Han, M.; Xie, S.L.; Bao, J.C.; Dai, Z.H.; Lan, Y.Q. Self-Assembly of a Mesoporous ZnS/Mediating Interface/CdS Heterostructure with Enhanced Visible-Light Hydrogen-Production Activity and Excellent Stability. *Chem Sci* **2015**, *6*, 5263–5268, doi:10.1039/C5SC01586C.
2. Jiang, D.; Sun, Z.; Jia, H.; Lu, D.; Du, P. A Cocatalyst-Free CdS Nanorod/ZnS Nanoparticle Composite for High-Performance Visible-Light-Driven Hydrogen Production from Water. *J Mater Chem A Mater* **2015**, *4*, 675–683, doi:10.1039/C5TA07420G.
3. Wang, X.; Li, X. yan Heterostruture CdS/ZnS Nanoparticles as a Visible Light-Driven Photocatalyst for Hydrogen Generation from Water. *Int J Green Energy* **2016**, *13*, 1201–1208, doi:10.1080/15435075.2016.1175349/SUPPL_FILE/LJGE_A_1175349_SM6365.DOC.
4. Wang, J.; Wang, Z.; Li, L.; Chen, J.; Zheng, J.; Jia, S.; Zhu, Z. Structure-Controlled CdS(0D, 1D, 2D) Embedded onto 2D ZnS Porous Nanosheets for Highly Efficient Photocatalytic Hydrogen Generation. *RSC Adv* **2017**, *7*, 24864–24869, doi:10.1039/C7RA02565C.
5. Kundu, J.; Satpathy, B.K.; Pradhan, D. Composition-Controlled CdS/ZnS Heterostructure Nanocomposites for Efficient Visible Light Photocatalytic Hydrogen Generation. *Ind Eng Chem Res* **2019**, *58*, 22709–22717, doi:10.1021/ACS.IECR.9B03764/ASSET/IMAGES/LARGE/IE9B03764_0001.jpeg.
6. Zhu, Y.; Jiang, X.; Lin, L.; Wang, S.; Chen, C. Fabrication of ZnS/CdS Heterojunction by Using Bimetallic MOFs Template for Photocatalytic Hydrogen Generation. *Chem Res Chin Univ* **2020**, *36*, 1032–1038, doi:10.1007/S40242-020-0083-5/METRICS.
7. Huang, L.; Wang, X.; Yang, J.; Liu, G.; Han, J.; Li, C. Dual Cocatalysts Loaded Type i CdS/ZnS Core/Shell Nanocrystals as Effective and Stable Photocatalysts for H₂ Evolution. *Journal of Physical Chemistry C* **2013**, *117*, 11584–11591, doi:10.1021/JP400010Z/SUPPL_FILE/JP400010Z_SI_001.PDF.
8. Xie, Y.P.; Yu, Z.B.; Liu, G.; Ma, X.L.; Cheng, H.M. CdS–Mesoporous ZnS Core–Shell Particles for Efficient and Stable Photocatalytic Hydrogen Evolution under Visible Light. *Energy Environ Sci* **2014**, *7*, 1895–1901, doi:10.1039/C3EE43750G.
9. Lin, Y.; Zhang, Q.; Li, Y.; Liu, Y.; Xu, K.; Huang, J.; Zhou, X.; Peng, F. The Evolution from a Typical Type-I CdS/ZnS to Type-II and Z-Scheme Hybrid Structure for Efficient and Stable Hydrogen Production under Visible Light. *ACS Sustain Chem Eng* **2020**, *8*, 4537–4546, doi:10.1021/ACSSUSCHEMENG.0C00101/ASSET/IMAGES/LARGE/SC0C00101_0003.jpeg.
10. Reddy, N.L.; Rao, V.N.; Kumari, M.M.; Sathish, M.; Muthukonda Venkatakrishnan, S. Development of High Quantum Efficiency CdS/ZnS Core/Shell Structured Photocatalyst for the Enhanced Solar Hydrogen Evolution. *Int J Hydrogen Energy* **2018**, *43*, 22315–22328, doi:10.1016/J.IJHYDENE.2018.10.054.
11. Ma, D.; Shi, J.W.; Sun, L.; Sun, Y.; Mao, S.; Pu, Z.; He, C.; Zhang, Y.; He, D.; Wang, H.; et al. Knack behind the High Performance CdS/ZnS-NiS Nanocomposites: Optimizing Synergistic Effect

between Cocatalyst and Heterostructure for Boosting Hydrogen Evolution. *Chemical Engineering Journal* **2022**, *431*, 133446, doi:10.1016/J.CEJ.2021.133446.

12. Hong, E.; Kim, D.; Kim, J.H. Heterostructured Metal Sulfide (ZnS–CuS–CdS) Photocatalyst for High Electron Utilization in Hydrogen Production from Solar Water Splitting. *Journal of Industrial and Engineering Chemistry* **2014**, *20*, 3869–3874, doi:10.1016/J.JIEC.2013.12.092.
13. Liu, M.; Wang, L.; Lu, G.; Yao, X.; Guo, L. Twins in Cd_{1-x}ZnxS Solid Solution: Highly Efficient Photocatalyst for Hydrogen Generation from Water. *Energy Environ Sci* **2011**, *4*, 1372–1378, doi:10.1039/C0EE00604A.
14. Liu, M.; Jing, D.; Zhou, Z.; Guo, L. Twin-Induced One-Dimensional Homojunctions Yield High Quantum Efficiency for Solar Hydrogen Generation. *Nature Communications* **2013** *4:1* **2013**, *4*, 1–8, doi:10.1038/ncomms3278.